

1 **Greenhouse gas fluxes in mangrove forest soil in an Amazon estuary**

2 Saúl Edgardo Martínez Castellón¹, José Henrique Cattanio^{1*}, José Francisco Berrêdo^{1,3},
3 Marcelo Rollnic², Maria de Lourdes Ruivo^{1,3}, Carlos Noriega².

4 ¹ Graduate Program in Environmental Sciences. Federal University of Pará, Belém,
5 Brazil

6 ² Marine Environmental Monitoring Research Laboratory. Federal University of Pará,
7 Belém, Brazil.

8 ³ Department of Earth Sciences and Ecology. Paraense Emílio Goeldi Museum, Belém,
9 Brazil

10 * Corresponding author: cattanio@ufpa.br (J.H. Cattanio)

11 Abstract: Tropical mangrove forests are important carbon sinks, the soil being the main
12 carbon reservoir. Understanding the variability and the key factors that control fluxes is
13 critical to accounting for greenhouse gas (GHG) emissions, particularly in the current
14 scenario of global climate change. This study is the first to quantify carbon dioxide
15 (CO_2) and methane (CH_4) emissions using a dynamic chamber in a natural mangrove
16 soil of the Amazon. The plots for the trace gases study were allocated at contrasting
17 topographic heights. The results showed that the mangrove soil of the Amazon estuary
18 is a source of CO_2 ($6.66 \text{ g CO}_2 \text{ m}^{-2} \text{ d}^{-1}$) and CH_4 ($0.13 \text{ g CH}_4 \text{ m}^{-2} \text{ d}^{-1}$) to the atmosphere.
19 The CO_2 flux was higher in the high topography ($7.86 \text{ g CO}_2 \text{ m}^{-2} \text{ d}^{-1}$) than in the low
20 topography ($4.73 \text{ g CO}_2 \text{ m}^{-2} \text{ d}^{-1}$) in the rainy season, and CH_4 was higher in the low
21 topography ($0.13 \text{ g CH}_4 \text{ m}^{-2} \text{ d}^{-1}$) than in the high topography ($0.01 \text{ g CH}_4 \text{ m}^{-2} \text{ d}^{-1}$) in the
22 dry season. However, in the dry period, the low topography soil produced more CH_4 .
23 Soil organic matter, carbon and nitrogen ratio (C/N), and redox potential influenced the
24 annual and seasonal variation of CO_2 emissions; however, they did not affect CH_4
25 fluxes. The mangrove soil of the Amazon estuary produced $35.40 \text{ Mg CO}_{2\text{-eq}} \text{ ha}^{-1} \text{ y}^{-1}$. A
26 total of $2.16 \text{ kg CO}_2 \text{ m}^{-2} \text{ y}^{-1}$ needs to be sequestered by the mangrove ecosystem to
27 counterbalance CH_4 emissions.

28 **1 Introduction**

29 Mangrove areas are estimated to be the main contributors to greenhouse gas emissions
30 in marine ecosystems (Allen et al., 2011; Chen et al., 2012). However, mangrove forests
31 are highly productive due to a high nutrient turnover rate (Robertson et al., 1992) and
32 have mechanisms that maximize carbon gain and minimize water loss through plant
33 transpiration (Alongi and Mukhopadhyay, 2015). A study conducted in 25 mangrove
34 forests (between 30° latitude and 73° longitude) revealed that these forests are the

35 richest in carbon (C) storage in the tropics, containing on average 1,023 Mg C ha⁻¹ of
36 which 49 to 98% is present in the soil (Donato et al., 2011).

37 The estimated soil CO₂ flux in tropical estuarine areas is 16.2 Tg C y⁻¹ (Alongi, 2009).
38 However, soil efflux measurements from tropical mangroves revealed emissions
39 ranging from 2.9 to 11.0 g CO₂ m⁻² d⁻¹ (Castillo et al., 2017; Chen et al., 2014; Shiu
40 and Chiu, 2020). In situ CO₂ production is related to the water input of terrestrial,
41 riparian, and groundwater brought by rainfall (Rosentreter et al., 2018b). Due to the
42 periodic tidal movement, the mangrove ecosystem is daily flooded, leaving the soil
43 anoxic and consequently reduced, favoring methanogenesis (Dutta et al., 2013). Thus,
44 estuaries are considered hotspots for CH₄ production and emission (Bastviken et al.,
45 2011; Borges et al., 2015). Organic material decomposition by methanogenic bacteria in
46 anoxic environments, such as sediments, inner suspended particles, zooplankton gut
47 (Reeburgh, 2007; Valentine, 2011), and the impact of freshwater should change the
48 electron flow from sulfate-reducing bacteria to methanogenesis (Purvaja et al., 2004),
49 which also results in CH₄ formation. On the other hand, high salinity levels, above 18
50 ppt, may result in an absence of CH₄ emissions (Poffenbarger et al., 2011), since CH₄
51 dissolved in pores is typically oxidized anaerobically by sulfate (Chuang et al., 2016).
52 Currently the uncertainty in emitted CH₄ values in vegetated coastal wetlands is
53 approximately 30% (EPA, 2017). Soil flux measurements from tropical mangroves
54 revealed emissions range from 0.3 to 4.4 mg CH₄ m⁻² d⁻¹ (Castillo et al., 2017; Chen et
55 al., 2014; Kreuzwieser et al., 2003).

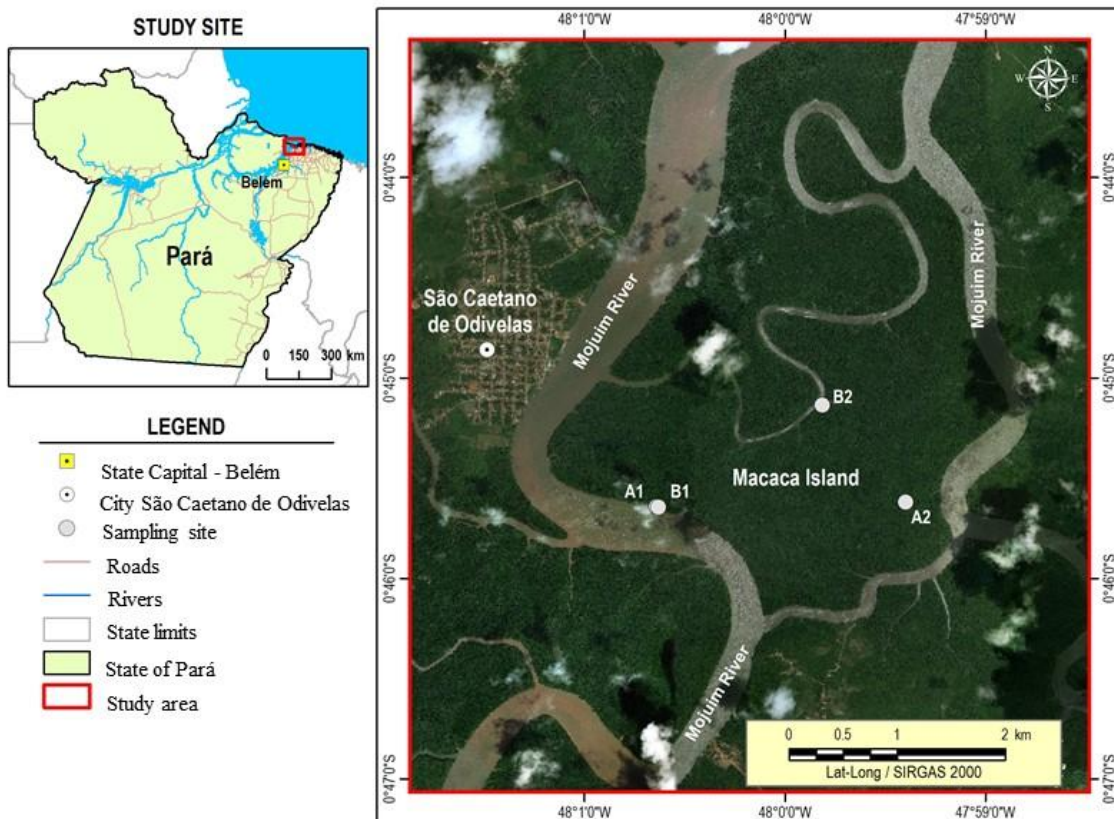
56 The production of greenhouse gases from soils is mainly driven by biogeochemical
57 processes. Microbial activities and gas production are related to soil properties,
58 including total carbon and nitrogen concentrations, moisture, porosity, salinity, and
59 redox potential (Bouillon et al., 2008; Chen et al., 2012). Due to the dynamics of tidal
60 movements, mangrove soils may become saturated and present reduced oxygen
61 availability, or suffer total aeration caused by the ebb tide. Studies attribute soil carbon
62 flux responses to moisture perturbations because of seasonality and flooding events
63 (Banerjee et al., 2016), with fluxes being dependent on tidal extremes (high tide and low
64 tide), and flood duration (Chowdhury et al., 2018). In addition, phenolic compounds
65 inhibit microbial activity and help keep organic carbon intact, thus leading to the
66 accumulation of organic matter in mangrove forest soils (Friesen et al., 2018).

67 The Amazonian coastal areas in the State of Pará (Brazil) cover 2,176.8 km² where
68 mangroves develop under the macro-tide regime (Souza Filho, 2005), representing
69 approximately 85% of the entire area of Brazilian mangroves (Herz, 1991). The
70 objective of this study is to investigate the monthly flux of CO₂ and CH₄ from the soil,
71 at two topographic heights, in a pristine mangrove area in the Mojuim River Estuary,
72 belonging to the Amazon biome. The gas fluxes were studied together with the analysis
73 of the vegetation structure and soil physical-chemical parameters.

74 **2 Material and Methods**

75 **2.1 Study site**

76 This study was conducted in the Amazonian coastal zone, Macaca Island (-0.746491
77 latitude and -47.997219 longitude), located in the Mojuim River estuary, at the
78 Mocapajuba Marine Extractive Reserve, municipality of São Caetano de Odivelas
79 (Figure 1), state of Pará (Brazil). The Macaca island has an area of 1,322 ha of pristine
80 mangroves, and belongs to a mangrove area of 2,177 km² in the state of Pará (Souza
81 Filho, 2005). The climate is type Am (tropical monsoon) according to the Köppen
82 classification (Peel et al., 2007). The climatological data were obtained from the
83 Meteorological Database for Teaching and Research of the National Institute of
84 Meteorology (INMET). The area has a rainy season from January to June (2,296 mm of
85 precipitation) and a dry season from July to December (687 mm). March and April were
86 the雨iest months with 505 and 453 mm of precipitation, while October and November
87 were the driest (53 and 61 mm, respectively). The minimum temperatures occur in the
88 rainy period (26 °C) and the maximum in the dry period (29 °C). The Mojuim estuary
89 has a macrotidal regime, with an average amplitude of 4.9 m during spring tide and 3.2
90 m during low tide (Rollnic et al., 2018). During the wet season the Mojuim River has a
91 flow velocity of 1.8 m s⁻¹ at the ebb tide and 1.3 m s⁻¹ at the flood tide, whereas in the
92 dry season, the maximum currents reach 1.9 m s⁻¹ at the flood and 1.67 m s⁻¹ at the ebb
93 tide (Rocha, 2015). The annual mean salinity of the river water is 26.95 PSU (Valentim
94 et al., 2018).



95

96 Figure 1. The Macaca Island located in the mangrove coast of Northern Brazil,
 97 Municipality of São Caetano de Odivelas (state of Pará), with sampling points at low
 98 (plot B1 and plot B2) and high (plot A1 and plot A2) topographies. Image Source: ©
 99 Google Earth

100 The Mojuim River region is geomorphologically formed by partially submerged river
 101 basins consequent of the increase in the relative sea level during the Holocene (Prost et
 102 al., 2001) associated with the formation of mangroves, dunes, and beaches (El-Robrini
 103 et al., 2006). Before reaching the estuary, the Mojuim River crosses an area of a dryland
 104 forest highly fragmented by family farming, forming remnants of secondary forest (<
 105 5.0 ha) of various ages (Fernandes and Pimentel, 2019). The population economically
 106 exploited the estuary, primarily by artisanal fishing, crab (*Ucides cordatus* L.)
 107 extraction, and oyster farms.

108 The flora of the mangrove area of Macaca Island is little anthropized and comprises the
 109 plant genera *Rhizophora*, *Avicenia*, *Laguncularia*, and *Acrostichum* (Ferreira, 2017;
 110 França et al., 2016). The estuarine plains are influenced by macrotide dynamics and can
 111 be physiographically divided into four sectors according to the different vegetation
 112 covers, associated with the landforms distribution, topographic gradient, tidal

113 inundation, and levels of anthropic transformation(França et al., 2016). The Macaca
114 Island is ranked as being from the fourth sector, which implies having woods of adult
115 trees of the genus *Ryzophora* with an average height of 10 to 25 m, is located at an
116 elevation of 0 to 5 m, and having silt-clay soil (França et al., 2016).

117 Four sampling plots were selected in the Macaca Island (Figure 1) on 19/05/2017, when
118 the moon was in the waning quarter phase: two plots where flooding occurs every day
119 (plots B1 and B2; Figure 1), called low topography (Top_Low), and two plots where
120 flooding occurs only at high tides during the solstice and on the high tides of the rainy
121 season of the new and full moons (plots A1 and A2; Figure 1), called high topography
122 (Top_High).

123 **2.2 Greenhouse gas flux measurements**

124 In each plot, eight Polyvinyl Chloride rings with 0.20 m diameter and 0.12 m height
125 were randomly installed within a circumference with a diameter of 20 m. The rings had
126 an area of 0.028 m² (volume of 3.47 L), were fixed 0.05 m into the ground, and
127 remained in place until the study was completed. Once a month, gas fluxes were
128 measured during periods of waning or crescent moon, as these are the times when the
129 soil in the low topography is more exposed. To avoid the influence of mangrove roots
130 on the gas fluxes, the rings were placed in locations without any seedlings or
131 aboveground mangrove roots. The CO₂ and CH₄ concentrations (ppm) were measured
132 using the dynamic chamber methodology (Norman et al., 1997; Verchot et al., 2000),
133 sequentially connected to a Los Gatos Research portable gas analyzer (Mahesh et al.,
134 2015). The device was calibrated monthly with a high quality standard gas (500 ppm
135 CO₂; 5 ppm CH₄). The rings were sequentially closed for three minutes with a PVC cap,
136 being connected to the analyzer through two 12.0 m polyethylene hoses. The gas
137 concentration was measured every two seconds and automatically stored by the
138 analyzer. CO₂ and CH₄ fluxes were calculated from the linear regression of
139 increasing/decreasing CO₂ and CH₄ concentrations within the chamber, usually between
140 one and three minutes after the ring cover was placed (Frankignoulle, 1988; McEwing
141 et al., 2015). The flux is considered zero when the linear regression reaches an R² <
142 0.30 (Sundqvist et al., 2014). However, in our analyses, most regressions reached R² >
143 0.70, and the regressions were weak and considered zero in only 6% of the samples. At
144 the end of each flux measurement, the height of the ring above ground was measured at

145 four equidistant points with a ruler. The seasonal data were analyzed by comparing the
146 average monthly fluxes in the wet season and dry season separately.

147 **2.3 Vegetation structure and biomass**

148 The floristic survey was conducted in October 2017 using circular 1,256.6 m² plots
149 (Kauffman et al., 2013) divided into four 314.15 m² subplots, which is the equivalent to
150 0.38 ha, at the same topographies as the gas flux analysis (Figure 1). We recorded the
151 diameter above the aerial roots, the diameter of the stem, and total height of all trees
152 with DBH (diameter at breast height; m) greater than 0.05m. The allometric equations
153 (Howard et al., 2014) to calculate tree biomass (aboveground biomass; AGB) were:
154 AGB = 0.1282 * DBH^{2.6} ($R^2 = 0.92$) for *R. mangle*; AGB = 0.140 * DBH^{2.4} ($R^2 = 0.97$)
155 for *A. germinans*; and Total AGB = 0.168 * ρ * DBH^{2.47} ($R^2 = 0.99$), where $\rho_{R. mangle} =$
156 0.87; $\rho_{A. germinans} = 0.72$ (ρ = wood density).

157 **2.4 Soil sampling and environmental characterization**

158 Four soil samples were collected with an auger at a depth of 0.10 m in all the studied
159 plots for gas flux measurements (Figure 1) in July 2017 (beginning of the dry season)
160 and January 2018 (beginning of the rainy season). Before the soil samples were
161 removed, pH and redox potential (Eh; mV) were measured with a Metrohm 744
162 equipment by inserting the platinum probe directly into the intact soil at a depth of 0.10
163 m (Bauza et al., 2002). The soil samples collected in the field were transported to the
164 laboratory (Chemical Analysis Laboratory of the *Museu Paraense Emílio Goeldi*) in
165 thermal boxes containing ice. The soil samples were analyzed on the day after collection
166 at the laboratory, and the samples were kept in a freezer. Salinity (Sal; ppt) was
167 measured with PCE-0100, and soil moisture (Sm; %) by the residual gravimetric
168 method (EMBRAPA, 1997).

169 Organic Matter (OM; g kg⁻¹), Total Carbon (T_C; g kg⁻¹) and Total Nitrogen (T_N; g kg⁻¹)
170 were calculated by volumetry (oxidoreduction) using the Walkley-Black method
171 (Kalembasa and Jenkinson, 1973). Microbial carbon (C_{mic}; mg kg⁻¹) and microbial
172 nitrogen (N_{mic}; mg kg⁻¹) were determined through the 2.0 min of Irradiation-extraction
173 method of soil by microwave technique (Islam and Weil, 1998). Microwave heated soil
174 extraction proved to be a simple, fast, accurate, reliable, and safe method to measure
175 soil microbial biomass (Araujo, 2010; Ferreira et al., 1999; Monz et al., 1991). The C_{mic}
176 was determined by dichromate oxidation (Kalembasa and Jenkinson, 1973; Vance et al.,

177 The N_{mic} was analyzed following the method described by Brookes et al. (1985),
178 changing fumigation to irradiation, which uses the difference between the amount of T_N
179 in irradiated and non-irradiated soil. We used the flux conversion factor of 0.33
180 (Sparling and West, 1988) and 0.54 (Almeida et al., 2019; Brookes et al., 1985), for
181 carbon and nitrogen, respectively. Particle size analysis was performed separately on
182 four soil samples collected at each flux plot, in the two seasons (October 2017 and
183 March 2018), according to EMBRAPA (1997).

184 At each gas flux measurement, environmental variables such as air temperature (T_{air} ,
185 °C), relative humidity (RH, %), and wind speed (W_s , m s⁻¹) were quantified with a
186 portable thermo-hygrometer (model AK821) at the height of 2.0 m above the soil
187 surface. Soil temperature (T_s , °C) was measured with a portable digital thermometer
188 (model TP101) after each gas flux measurement. Daily precipitation was obtained from
189 an automatic precipitation station installed at a pier on the banks of the Mojuim River in
190 São Caetano das Odivelas (coordinates: -0.738333 latitude; -48.013056 longitude).

191 **2.5 Statistical analyses**

192 On the Macaca Island, two treatments were allocated (low and high topography), with
193 two plots in either treatment. In each plot, eight chambers were randomly distributed,
194 which were considered sample repetitions. The normality of the data of CH_4 and FCO_2
195 flux, and soil physicochemical parameters was evaluated using the Shapiro-Wilks
196 method. The soil CO_2 and CH_4 flux showed a non-normal distribution. Therefore, we
197 used the non-parametric ANOVA (Kruskal-Wallis, $p < 0.05$) to test the differences
198 between the two treatments among months and seasons. The physicochemical
199 parameters were normally distributed. Therefore, a parametric ANOVA was used to test
200 the statistical differences ($p < 0.05$) between the two treatments among months and
201 seasons. Pearson correlation coefficients were calculated to determine the relationships
202 between soil properties and gas fluxes in the months (dry and wet season) when the
203 chemical properties of the soil were analyzed at the same time as gas fluxes were
204 measured. Statistical analyses were performed with the free statistical software Infostat
205 2015®.

206

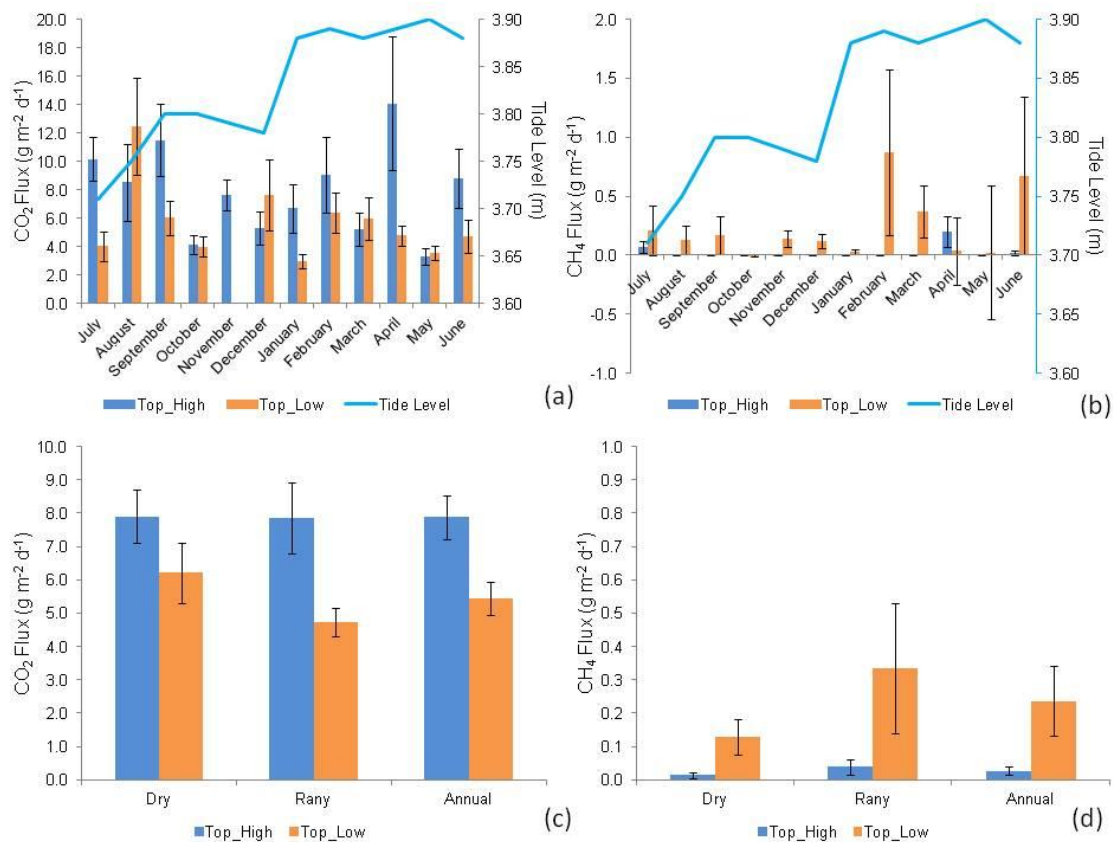
3 Results

207

3.1 Carbon dioxide and methane fluxes

208 CO₂ fluxes differed significantly between topographies only in January (H = 3.915; p =
 209 0.048), July (H = 9.091; p = 0.003), and November (H = 11.294; p < 0.001) (Figure 2;
 210 Supplementary Information, SI 1), with generally higher fluxes at the high topography
 211 than at the low topography. At the high topography, CO₂ fluxes were significantly
 212 higher (H = 24.510; p = 0.011) in July compared to August and December, March,
 213 October, and May, not differing from the other months of the year. Similarly, at the low
 214 topography, CO₂ fluxes were statistically higher (H = 19.912; p = 0.046) in September
 215 and February than in January and November, not differing from the other months. We
 216 found a mean monthly flux of 7.9 ± 0.7 g CO₂ m⁻² d⁻¹ (mean \pm standard error) and $5.4 \pm$
 217 0.5 g CO₂ m⁻² d⁻¹ at the high and low topographies, respectively.

218



219

220 Figure 2. CO₂ (a) and CH₄ (b) fluxes (g CO₂ or CH₄ m⁻² d⁻¹) monthly (July 2018 to June
 221 2019) (n = 16). Seasonal (Dry and Rainy) and annual fluxes of CO₂ (c) and CH₄ (d), at

222 high (Top_High) and low (Top_Low) topographies ($n = 96$), in a mangrove forest soil
223 compared to tide level (Tide Level). The bars represent the standard error of the mean.

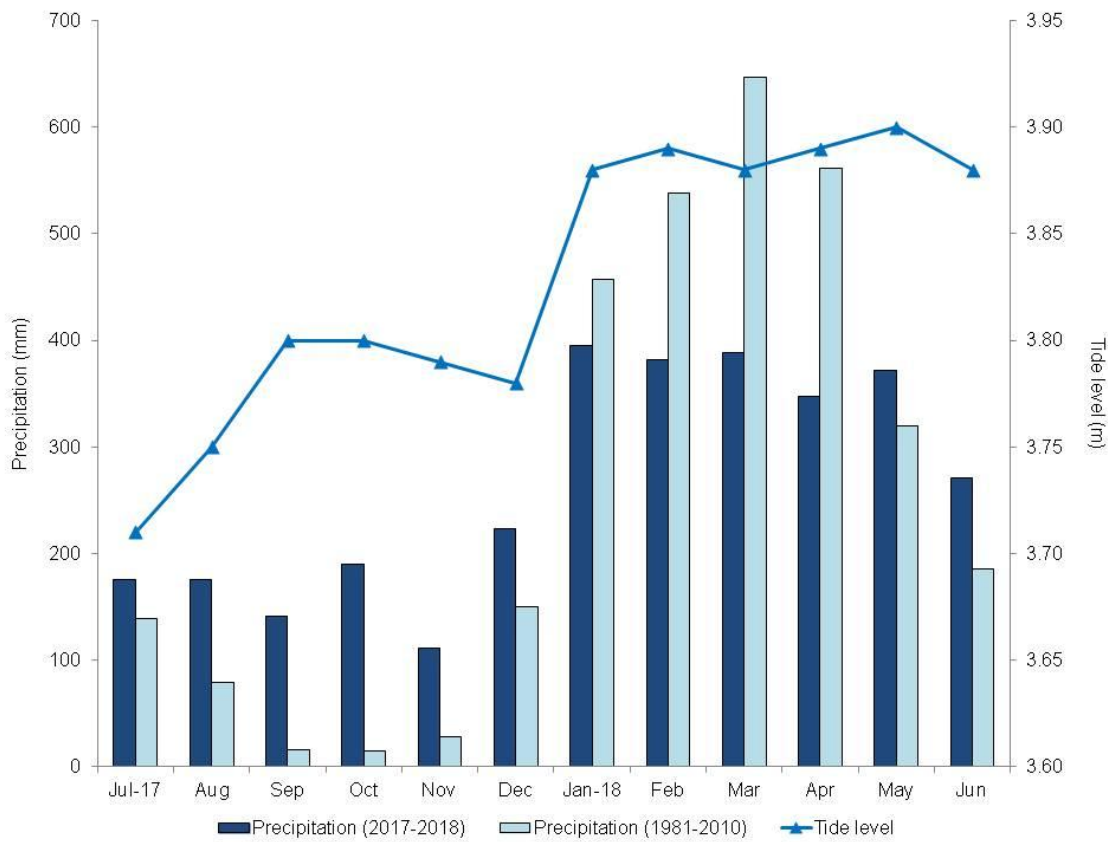
224 The CH_4 fluxes were statistically different between topographies only in November (H
225 = 9.276; $p = 0.002$) and December ($H = 4.945$; $p = 0.005$), with higher fluxes at the low
226 topography (Figure 2; SI 1). At the high topography, CH_4 fluxes were significantly ($H =$
227 40.073; $p < 0.001$) higher in April and July compared to the other months studied, and
228 in November CH_4 was consumed from the atmosphere (Figure 2; SI 1). Similarly, CH_4
229 fluxes at the low topography did not vary significantly among months ($H = 10.114$; $p =$
230 0.407).

231 Greenhouse gas fluxes (Figure 2) were only significantly different between
232 topographies in the dry season (Figure 3), period when CO_2 fluxes were higher ($H =$
233 7.378; $p = 0.006$) at the high topography and CH_4 fluxes at the low topography ($H =$
234 8.229; $p < 0.001$). In the Macaca Island, the mean annual fluxes of CO_2 and CH_4 were
235 $6.659 \pm 0.419 \text{ g CO}_2 \text{ m}^{-2} \text{ d}^{-1}$ and $0.132 \pm 0.053 \text{ g CH}_4 \text{ m}^{-2} \text{ d}^{-1}$, respectively. During the
236 study year, the CO_2 flux from the mangrove soil ranged from -5.06 to $68.96 \text{ g CO}_2 \text{ m}^{-2}$
237 d^{-1} (mean $6.66 \text{ g CO}_2 \text{ m}^{-2} \text{ d}^{-1}$), while the CH_4 flux ranged from -5.07 to $11.08 \text{ g CH}_4 \text{ m}^{-2}$
238 d^{-1} (mean $0.13 \text{ g CH}_4 \text{ m}^{-2} \text{ d}^{-1}$), resulting in a total carbon rate of $1.92 \text{ g C m}^{-2} \text{ d}^{-1}$ or 7.00
239 $\text{Mg C ha}^{-1} \text{ y}^{-1}$ (Figure 2).

240 **3.2 Weather data**

241 There was a marked seasonality during the study period (Figure 2), with 2,155.0 mm of
242 precipitation during the rainy period and 1,016.5 mm during the dry period. The highest
243 tides occurred in the period of greater precipitation (Figure 3) due to the rains. However,
244 the rainfall distribution was different from the climatological normal (Figure 3). The
245 precipitation in the rainy season was 553.2 mm below and in the dry season was 589.1
246 mm above the climatological normal. Thus, in the period studied, the dry season was
247 rainier and the rainy season drier than the climatological normal, which may be a
248 consequence of the La Niña event (Wang et al., 2019).

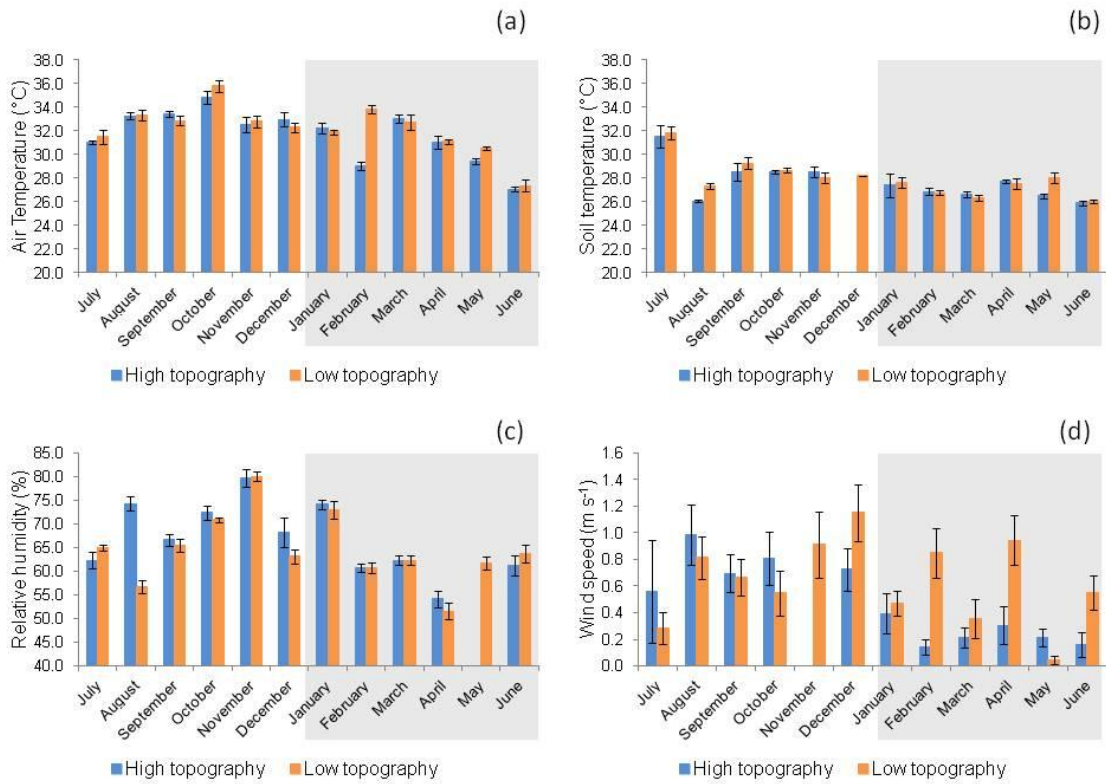
249



250

251 Figure 3. Monthly climatological normal in the municipality of Soure (1981-2010, mm),
 252 monthly precipitation (mm), and maximum tide height (m) from 2017 to 2018, in the
 253 municipality of São Caetano de Odivelas (PA).

254 T_{air} was significantly higher ($LSD = 0.72$, $p = 0.01$) at the high (31.24 ± 0.26 $^{\circ}C$) than at
 255 the low topography (30.30 ± 0.25 $^{\circ}C$) only in the rainy season (Figure 4a). No
 256 significant variation in T_s was found between topographies in either season (Figure 4b).
 257 RH was significantly higher ($LSD = 2.55$, $p = 0.01$) at the high topography ($70.54 \pm$
 258 0.97%) than at the low topography ($66.85 \pm 0.87\%$) only in the rainy season (Figure 4c).
 259 W_s (Figure 4d) was significantly higher ($LSD = 0.15$, $p < 0.00$) at the low (0.54 ± 0.06
 260 $m s^{-1}$) than at the high topography ($0.24 \pm 0.04 m s^{-1}$) also in the rainy season.



261

262 Figure 4. a) Air temperature (°C), b) soil temperature (°C), c) relative humidity (%), and
 263 d) wind speed (m s^{-1}) at high and low topographies, from July 2017 to June 2018 in a
 264 mangrove area in the Mojuim River estuary. Bars highlighted in grey correspond to the
 265 rainy season ($n = 16$). The bars represent the standard error.

266 3.3 Soil characteristics

267 Silt concentration was higher at the low topography (LSD: 14.763; $p = 0.007$) and clay
 268 concentration was higher at the high topography plots (LSD: 12.463; $p = 0.005$), in both
 269 seasons studied (Table 1). Soil particle size analysis did not differ statistically ($p > 0.05$)
 270 between the two seasons (Table 1). Soil moisture did not vary significantly ($p > 0.05$)
 271 between topographies at each season, or between seasonal periods at the same
 272 topography (Table 1). The pH varied statistically (LSD: 5.950; $p = 0.006$) only at the
 273 low topography when the two seasons were compared, being more acidic in the dry
 274 period (Table 1). The pH values were significantly (LSD: 0.559; $p = 0.008$) higher in the
 275 dry season (Table 1). No variation in Eh was identified between topographies and
 276 seasons (Table 1), although it was higher in the dry season than in the rainy season.
 277 However, Sal values were higher (LSD: 3.444; $p = 0.010$) at the high topography than at
 278 the low topography in the dry season (Table 1). In addition, Sal was significantly higher

279 in the dry season than in the rainy season, in both high (LSD: 2.916; $p < 0.001$) and low
280 (LSD: 3.003; $p < 0.001$) topographies (Table 1).

281 Table 1. Analysis of Sand (%), Silt (%), Clay (%), Moisture (%), pH, Redox Potential (Eh, mV) and salinity (Sal; ppt) in the mangrove soil of
 282 high and low topographies, and in the rainy and dry seasons (Macaca island, São Caetano das Odivelas). Numbers represent the mean \pm standard
 283 error of the mean. Lower case letters compare topographies in each seasonal period and upper-case letters compare the same topography between
 284 seasonal periods. Different letters indicate statistical difference (LSD, $p < 0.05$).

Season	Topography	Sand (%)	Silt (%)	Clay (%)	Moisture (%)	pH	Eh (mV)	Sal (ppt)
Dry	High	12.1 \pm 1.4 ^{aA}	41.8 \pm 3.3 ^{bA}	46.1 \pm 2.6 ^{aA}	73.1 \pm 6.6 ^{aA}	5.5 \pm 0.2 ^{aA}	190.25 \pm 45.53 ^{aA}	35.25 \pm 1.11 ^{aA}
	Low	9.7 \pm 2.5 ^{aA}	63.6 \pm 6.1 ^{aA}	26.6 \pm 5.2 ^{bA}	86.9 \pm 3.4 ^{aA}	5.3 \pm 0.3 ^{aA}	106.38 \pm 53.76 ^{aA}	30.13 \pm 1.16 ^{bA}
	Mean	10.9 \pm 1.4 ^A	52.7 \pm 4.4 ^A	36.4 \pm 3.8 ^A	80.0 \pm 4.0 ^A	5.4 \pm 0.2 ^A	148.31 \pm 35.71 ^A	32.69 \pm 1.02 ^A
Rainy	High	12.4 ^{aA} 3 ^{aA}	41.8 ^{aA} 39.3 ^{bA}	46 ^{aA} 48.4 ^{aA} 21 ^{bA}	73 ^{aA}	88.9 \pm 3.5 ^{aA}	4.9 \pm 0.4 ^{aA}	92.50 \pm 56.20 ^{aA}
	Low	9.7 ^{aA} 8 ^{bA}	63.6 ^{aA} 45.1 ^{aA}	26 ^{aA} 28.6 ^{bA} 54 ^{bA}	88.6 \pm 3.7 ^{aA}	4.4 \pm 0.1 ^{aB}	36.25 \pm 49.97 ^{aA}	8.13 \pm 0.79 ^{aB}
	Mean	10.9 ^{aA} 1 ^{aA}	52.5 ^{aA} 1 ^{aA}	36 ^{aA} 38.4 ^{aA} 3.8 ^{bA}	88.7 \pm 2.5 ^A	4.6 \pm 0.2 ^B	64.38 \pm 37.04 ^A	7.81 \pm 0.54 ^B

286 The C_{mic} did not differ between topographies in the two seasons (Table 2). However, T_C
287 was significantly higher in the low topography in the dry season (LSD: 5.589; $p <$
288 0.000) and in the rainy season (LSD: 5.777; $p = 0.024$). In addition, C_{mic} was higher in
289 the dry season in both the high (LSD: 11.325; $p < 0.010$) and low (LSD: 9.345; $p <$
290 0.000) topographies (Table 2). N_{mic} did not vary between topographies seasonally.
291 However, N_{mic} in the high (LSD: 9.059; $p = 0.013$) and low topographies (LSD: 4.447;
292 $p = 0.001$) was higher during the dry season (Table 2). The C/N ratio (Table 2) was
293 higher in the low than in the high topography in both the dry (LSD: 3.142; $p < 0.000$)
294 and rainy seasons (LSD: 3.675; $p = 0.033$). However, only in the low topography was
295 the C/N ratio higher (LSD: 1.863; $p < 0.000$) in the dry season than in the rainy season
296 (Table 2). Soil OM was higher at the low topography in the rainy (LSD: 9.950; $p =$
297 0.024) and in the dry seasons (LSD: 9.630; $p < 0.000$). Only in the lowland topography
298 was the OM concentration higher in the dry season than in the rainy season (Table 2).

299 Table 2. Seasonal and topographic variation in microbial Carbon (C_{mic}; mg kg⁻¹), microbial Nitrogen (N_{mic}, mg kg⁻¹), Total Carbon (T_C; g kg⁻¹),
 300 Total Nitrogen (N_T; g kg⁻¹), Carbon/Nitrogen ratio (C/N) and Soil Organic Matter (OM; g kg⁻¹). Numbers represent the mean (±standard error).
 301 Lower case letters compare topographies at each season, and upper-case letters compare the topography between seasons.

Season	Topography	C _{mic}	N _{mic}	T _C	T _N	C/N	OM
		mg kg ⁻¹	mg kg ⁻¹	g kg ⁻¹	g kg ⁻¹		
Dry	High	22.12±5.22 ^{aA}	12.76±4.20 ^{aA}	14.12±2.23 ^{bA}	1.43±0.06 ^{aA}	9.60±1.20 ^{bA}	24.35±3.84 ^{bA}
	Low	26.34±4.23 ^{aA}	10.34±2.05 ^{aA}	26.44±1.35 ^{aA}	1.56±0.04 ^{aA}	16.98±0.84 ^{aA}	45.59±2.32 ^{aA}
	Mean	24.23±3.29 ^A	11.55±2.28 ^A	20.28 ±2.03 ^A	1.49±0.04 ^A	13.29±1.19 ^A	34.97±3.50 ^A
Rainy	High	7.40±0.79 ^{aB}	0.75±0.41 ^{aB}	11.46±2.48 ^{bA}	1.32±0.04 ^{aA}	8.42±1.70 ^{bA}	19.75±4.27 ^{bA}
	Low	5.95±1.06 ^{aB}	1.23±0.28 ^{aB}	18.27±1.06 ^{aB}	1.46±0.06 ^{aA}	12.47±0.22 ^{aB}	31.51±1.83 ^{aB}
	Mean	6.68±0.67 ^B	0.99±0.25 ^B	14.86 ±1.57 ^B	1.39±0.04 ^A	10.44±0.98 ^A	25.63±2.71 ^B

302

303 **3.4 Vegetation structure and biomass**

304 Only the species *R. mangle* and *A. germinans* were found in the floristic survey carried
305 out. The DBH did not vary significantly between the topographies for either species
306 (Table 3). However, *R. mangle* had a higher DBH than *A. germinaris* at both high
307 (LSD: 139.304; p = 0.037) and low topographies (LSD: 131.307; p = 0.001). The basal
308 area (BA) and AGB did not show significant variation (Table 3). A total aboveground
309 biomass of $322.1 \pm 49.6 \text{ Mg ha}^{-1}$ was estimated.

310

311 Table 3: Summed Diameter at Breast Height (DBH; cm), Basal Area (BA; $m^2 ha^{-1}$) and Aboveground Biomass (AGB; $Mg ha^{-1}$) at high and low
 312 topographies in the mangrove forest of the Mojuim River estuary. Numbers represent the mean \pm standard error of the mean. Lower case letters
 313 compare topographic height for each species, and upper-case letters compare species at each topographic height, using Tukey's test ($p < 0.05$).

Species	Topography	N ha^{-1}	DBH	BA	AGB
			(cm)	($m^2 ha^{-1}$)	($Mg ha^{-1}$)
<i>Rhizophora</i>	High	302.4 \pm 20.5	238.8 \pm 24.9 ^{aA}	17.3 \pm 2.0 ^{aA}	219.3 \pm 25.7 ^{aA}
<i>mangle</i>	Low	310.4 \pm 37.6	283.5 \pm 45.0 ^{aA}	24.2 \pm 4.3 ^{aA}	338.7 \pm 62.9 ^{aA}
<i>Avicennia</i>	High	47.7 \pm 20.5	86.8 \pm 51.2 ^{aB}	13.8 \pm 9.2 ^{aA}	135.3 \pm 94.7 ^{aA}
<i>germinans</i>	Low	15.9 \pm 9.2	46.1 \pm 29.3 ^{aB}	11.8 \pm 8.8 ^{aA}	136.0 \pm 108.3 ^{aA}
Total	High	350.2 \pm 18.4	325.6 \pm 33.6 ^a	31.1 \pm 7.5 ^a	304.5 \pm 99.8 ^a
	Low	346.2 \pm 41.0	296.0 \pm 23.7 ^a	30.0 \pm 4.1 ^a	330.8 \pm 60.4 ^a

314 The equations for biomass estimates (AGB) were: $R. mangle = 0.1282 * DBH^{2.6}$; $A. germinans = 0.14 * DBH^{2.4}$; and Total = $0.168 * \rho * DBH^{2.47}$, where $\rho_{R. mangle} = 0.87$; $\rho_{A. germinans}$
 315 = 0.72 (Howard et al., 2014).

316

317 **3.5 Drivers of greenhouse gas fluxes**

318 In the rainy season, CO₂ efflux was correlated with T_{air} (Pearson = 0.23, p = 0.03), RH
319 (Pearson = -0.32, p < 0.00) and T_s (Pearson = 0.21, p = 0.04) only at the low
320 topography. In the dry season CO₂ flux was correlated with T_s (Pearson = 0.39, p <
321 0.00) at the low topography. The dry season was the period in which we found the
322 greatest amount of significant correlations between CO₂ efflux and soil chemical
323 parameters, while the C:N ratio, OM, and Eh were correlated with CO₂ efflux in both
324 seasons (Table 4). The negative correlation between T_C, N_T, C/N, and OM, along with
325 the positive correlation of N_{mic} with soil CO₂ flux, in the dry period, indicates that
326 microbial activity is a decisive factor for CO₂ efflux (Table 4). Soil moisture in the
327 Mojuim River mangrove forest negatively influenced CO₂ flux in both seasons (Table
328 4). However, soil moisture was not correlated with CH₄ flux. No significant correlations
329 were found between CH₄ efflux and the chemical properties of the soil in the mangrove
330 of the Mojuim River estuary (Table 4).

331

332 Table 4. Correlation coefficient (Pearson) of CO₂ and CH₄ fluxes with chemical parameters of the soil in a mangrove area in the Mojuim River
 333 estuary.

Gas Flux	Season	T _C (g m ⁻² d ⁻¹)	T _N (g kg ⁻¹)	C _{mic} (mg kg ⁻¹)	N _{mic} (mg kg ⁻¹)	C/N	OM (g kg ⁻¹)	Sal (ppt)	Eh (mV)	pH	Moisture (%)
CO ₂	Dry	-0.68 ^{**}	-0.59 [*]	0.18 ^{NS}	0.61 ^{**}	-0.66 ^{**}	-0.67 ^{**}	-0.07 ^{NS}	0.51 [*]	0.21 ^{NS}	-0.49 [*]
	Rainy	-0.44 ^{NS}	-0.20 ^{NS}	-0.15 ^{NS}	-0.32 ^{NS}	-0.50 [*]	-0.63 ^{**}	-0.54 [*]	0.53 [*]	0.47 ^{NS}	-0.54 [*]
	Annual	-0.50 ^{**}	-0.35 [*]	-0.18 ^{NS}	0.00 ^{NS}	-0.53 ^{**}	-0.48 ^{**}	-0.30 ^{NS}	0.39 [*]	0.23 ^{NS}	-0.56 ^{**}
CH ₄	Dry	0.30 ^{NS}	0.07 ^{NS}	-0.14 ^{NS}	-0.24 ^{NS}	0.34 ^{NS}	0.02 ^{NS}	-0.04 ^{NS}	-0.38 ^{NS}	0.26 ^{NS}	0.26 ^{NS}
	Rainy	0.05 ^{NS}	-0.09 ^{NS}	0.44 ^{NS}	-0.27 ^{NS}	0.09 ^{NS}	-0.11 ^{NS}	-0.04 ^{NS}	-0.13 ^{NS}	-0.07 ^{NS}	0.04 ^{NS}
	Annual	0.04 ^{NS}	-0.10 ^{NS}	-0.01 ^{NS}	-0.18 ^{NS}	0.08 ^{NS}	-0.01 ^{NS}	-0.17 ^{NS}	-0.21 ^{NS}	-0.08 ^{NS}	0.02 ^{NS}

334 Total Carbon (T_C; g kg⁻¹); Total Nitrogen (T_N; g kg⁻¹); Microbial Carbon (C_{mic}, g kg⁻¹); Microbial Nitrogen (N_{mic}, g kg⁻¹); Carbon and Nitrogen
 335 ratio (C/N); Organic Matter (OM; g kg⁻¹); Salinity (Sal; ppt); Redox Potential (Eh; mV); Soil Moisture (Moisture, %).

336 NS= not significant; * significant effects at p ≤ 0.05; ** significant effects at p ≤ 0.01

337

338 **4 Discussion**339 **4.1 Carbon dioxide and methane flux**

340 It is important to consider that the year under study was rainier in the dry season (2017)
341 and less rainy in the wet season (2018) when the climatological average is concerned
342 (1981-2010) (Figure 3). Perhaps this variation is related to the La Niña effects, and the
343 intensification of extreme events is considered as global climate changes_(Gash et al.,
344 2004)—. Under these conditions, negative and positive fluxes of the two greenhouse
345 gases were found (negative values represent gas consumption). The negative CO₂ flux is
346 apparently a consequence of the increased CO₂ solubility in tidal waters or of the
347 increased sulfate reduction, as described in the literature (Borges et al., 2018;
348 Chowdhury et al., 2018; Nóbrega et al., 2016). Fluctuations in redox potential altered
349 the availability of the terminal electron acceptor and donor, and the forces of recovery
350 of their concentrations in the soil, such that a disproportionate release of CO₂ can result
351 from the alternative anaerobic degradation processes such as sulfate and iron reduction
352 (Chowdhury et al., 2018). The soil carbon flux in the mangrove area in the Amazon
353 region was within the range of findings for other tropical mangrove areas (2.6 to 11.0 g
354 CO₂ m⁻² d⁻¹; Shiao and Chiu, 2020). However, the mean flux of 6.2 mmol CO₂ m⁻² h⁻¹
355 recorded in this Amazonian mangrove was much higher than the mean efflux of 2.9
356 mmol CO₂ m⁻² h⁻¹ recorded in 75 mangroves during low tide periods (Alongi, 2009).

357 An emission of 0.01 Tg CH₄ y⁻¹, 0.6 g CH₄ m⁻² d⁻¹ (Rosentreter et al., 2018a), or 26.7
358 mg CH₄ m⁻² h⁻¹ has been reported for tropical latitudes (0 and 5°). In our study, the
359 monthly average of CH₄ flux was higher at the low (7.3 ± 8.0 mg CH₄ m⁻² h⁻¹) than at
360 the high topography (0.9 ± 0.6 mg C m⁻² h⁻¹), resulting in 0.1 g CH₄ m⁻² d⁻¹ or 0.5 Mg
361 CH₄ ha⁻¹ y⁻¹ (Figure 2). Therefore, the CH₄-C fluxes from the mangrove soil in the
362 Mojuim River estuary were much lower than expected. It is known that there is a
363 microbial functional module for CH₄ production and consumption (Xu et al., 2015) and
364 diffusibility of CH₄ (Sihi et al., 2018), and this module considers three key mechanisms:
365 aceticlastic methanogenesis (acetate production), hydrogenotrophic methanogenesis (H₂
366 and CO₂ production), and aerobic methanotrophy (CH₄ oxidation and O₂ reduction).
367 The average emission from the soil of 8.4 mmol CH₄ m⁻² d⁻¹ was well below the fluxes
368 recorded in the Bay of Bengal, with 18.4 mmol CH₄ m⁻² d⁻¹ (Biswas et al., 2007). In the
369 Amazonian mangrove studied the mean annual carbon equivalent efflux was 429.6 mg
370 CO_{2-eq} m⁻² h⁻¹. This value is insignificant compared to the projected erosion losses of

371 103.5 Tg CO₂-eq ha⁻¹ y⁻¹ for the next century in tropical mangrove forests (Adame et al.,
372 2021). These higher CO₂ flux concomitantly with lower CH₄ flux in this Amazonian
373 estuary are probably a consequence of changes in the rainfall pattern already underway,
374 where the dry season was wetter and the rainy season drier when compared to the
375 climatological normal. The most recent estimate between latitude 0° to 23.5° S shows
376 an emission of 2.3 g CO₂ m⁻² d⁻¹ (Rosentreter et al., 2018b). However, the efflux in the
377 mangrove of the Mojuim River estuary was 6.7 g CO₂ m⁻² d⁻¹. For the same latitudinal
378 range, Rosentreter et al. (2018c) estimated an emission of 0.6 g CH₄ m⁻² d⁻¹, and we
379 found an efflux of 0.1 g CH₄ m⁻² d⁻¹.

380 4.2 Drivers of greenhouse gas fluxes

381 Mangrove areas are periodically flooded, with a larger flood volume during the syzygy
382 tides, especially in the rainy season. The hydrological condition of the soil is determined
383 by the microtopography and can regulate the respiration of microorganisms (aerobic or
384 anaerobic), being a decisive factor in controlling the CO₂ efflux (Dai et al., 2012;
385 Davidson et al., 2000; Ehrenfeld, 1995). No significant influence on CO₂ flux was
386 observed due to the low variation in high tide level throughout the year (0.19 m) (Figure
387 2), although it was numerically higher at the high topography. However, tidal height
388 and the rainy season resulted in a higher CO₂ flux (rate high/low =1.7) at the high
389 topography (7.86 ± 0.04 g CO₂ m⁻² d⁻¹) than at the low topography (4.73 ± 0.34 g CO₂
390 m⁻² d⁻¹) (Figure 2; SI 1). This result may be due to the root systems of most flood-
391 tolerant plants remaining active when flooded (Angelov et al., 1996). Still, the high
392 topography has longer flood-free periods, which only happens when the tides are
393 syzygy or when the rains are torrential.

394 CO₂ efflux was higher in the high topography than in the low topography in the rainy
395 season (when soils are more subject to inundation), i.e., 39.8% lower in the forest soil
396 exposed to the atmosphere for less time. Measurements performed on 62 mangrove
397 forest soils showed an average flux of 2.87 mmol CO₂ m⁻² h⁻¹ when the soil was
398 exposed to the atmosphere, while 75 results on flooded mangrove forest soils showed an
399 average emission of 2.06 mmol CO₂ m⁻² h⁻¹ (Alongi, 2007, 2009), i.e., 28.2% less than
400 for the dry soil. This reflects the increased facility gases have for molecular diffusion
401 than fluids, and the increased surface area available for aerobic respiration and chemical
402 oxidation during air exposure (Chen et al., 2010). Some studies attribute this variation
403 to the temperature of the soil when it is exposed to tropical air (Alongi, 2009), which

404 increases the export of dissolved inorganic carbon (Maher et al., 2018). However,
405 although despite the lack of significant variation in soil temperature between
406 topographies at each time of year (Figure 4b), there was a positive correlation (Pearson
407 = 0.15, $p = 0.05$) between CO_2 efflux and soil temperature at the low topography.

408 Some studies show that CH_4 efflux is a consequence of the seasonal temperature
409 variation in mangrove forest under temperate/monsoon climates (Chauhan et al., 2015;
410 Purvaja and Ramesh, 2001; Whalen, 2005). However, in your study CH_4 efflux was
411 correlated with Ta (Pearson = -0.33, $p < 0.00$) and RH (Pearson = 0.28, $p = 0.01$) only
412 in the dry season and at the low topography. The results show that the physical
413 parameters do not affect the fluxes in a standardized way, and their greater or lesser
414 influence depends on the topography and seasonality.

415 A compilation of several studies showed that the total CH_4 emissions from the soil in a
416 mangrove ecosystem range from 0 to $23.68 \text{ mg C m}^{-2} \text{ h}^{-1}$ (Shiau and Chiu, 2020), and
417 our study showed a range of -0.01 to $31.88 \text{ mg C m}^{-2} \text{ h}^{-1}$ (mean of $4.70 \pm 5.00 \text{ mg C m}^{-2}$
418 h^{-1}). The monthly CH_4 fluxes were generally higher at the low ($0.232 \pm 0.256 \text{ g CH}_4 \text{ m}^{-2}$
419 d^{-1}) than at the high ($0.026 \pm 0.018 \text{ g CH}_4 \text{ m}^{-2} \text{ d}^{-1}$) topography, especially during the
420 rainy season when the tides were higher (Figure 2). Only in the dry season was there a
421 significantly higher production at the low than at the high topography (Figure 2; SI 1).
422 The low topography produced $0.0249 \text{ g C m}^{-2} \text{ h}^{-1}$ more to the atmosphere in the rainy
423 season than in the dry season (Figure 2), and a similar seasonal pattern was recorded in
424 other studies (Cameron et al., 2021).

425 The mangrove soil in the Mojuim River estuary is rich in silt and clay (Table 1), which
426 reduces sediment porosity and fosters the formation and maintenance of anoxic
427 conditions (Dutta et al., 2013). In addition, the lack of oxygen in the flooded mangrove
428 soil favors microbial processes such as denitrification, sulfate reduction,
429 methanogenesis, and redox reactions (Alongi and Christoffersen, 1992). A significant
430 amount of CH_4 produced in wetlands is dissolved in the pore water due to high pressure,
431 causing supersaturation, which allows CH_4 to be released by diffusion from the
432 sediment to the atmosphere and by boiling through the formation of bubbles.

433 Studies show that the CO_2 flux tends to be lower with high soil saturation (Chanda et
434 al., 2014; Kristensen et al., 2008). A total of 395 Mg C ha^{-1} was found at the soil surface
435 (0.15 m) in the mangrove of the Mojuim River estuary, which was slightly higher than
436 the 340 Mg C ha^{-1} found in other mangroves in the Amazon (Kauffman et al., 2018),

437 however being significantly 1.8 times greater at the low topography (Table 2). The finer
438 soil texture at the low topography (Table 1) reduces groundwater drainage which
439 facilitates the accumulation of C in the soil (Schmidt et al., 2011).

440 4.3 Mangrove biomass

441 Only the species *R. mangle* and *A. germinans* were found in the floristic survey carried
442 out, which is aligned with the results of other studies in the same region (Menezes et al.,
443 2008). Thus, the variations found in the flux between the topographies in the Mojuim
444 River estuary are not related to the mangrove forest structure, because there was no
445 difference in the aboveground biomass. Since there was no difference in the species
446 composition, the belowground biomass is not expected to differ either (Table 3).

447 Assuming that the amount of carbon stored is 42.0% of the total biomass (Sahu and
448 Kathiresan, 2019), the mangrove forest biomass of the Mojuim River estuary stores
449 127.9 and 138.9 Mg C ha⁻¹ at the high and low topographies, respectively. This result is
450 lower than the 507.8 Mg C ha⁻¹ estimated for Brazilian mangroves (Hamilton and
451 Friess, 2018), but are near the 103.7 Mg C ha⁻¹ estimated for a mangrove at Guará's
452 island (Salum et al., 2020), 108.4 Mg C ha⁻¹ for the Bragantina region (Gardunho,
453 2017), and 132.3 Mg C ha⁻¹ in French Guiana (Fromard et al., 1998). Thus, the biomass
454 found in the Mojuim estuary does not differ from the biomass found in other
455 Amazonian mangroves. The estimated primary production for tropical mangrove forests
456 is 218 ± 72 Tg C y⁻¹ (Bouillon et al., 2008).

457 4.4 Biogeochemical parameters

458 During the seasonal and annual periods, CH₄ efflux was not significantly correlated
459 with chemical parameters (Table 5), ~~which is~~ similar to the as observed in another study
460 (Chen et al., 2010). Flooded soils present reduced gas diffusion rates, which directly
461 affects the physiological state and activity of microbes, by limiting the supply of the
462 dominant electron acceptors (e.g., oxygen), and gases (e.g., CH₄) (Blagodatsky and
463 Smith, 2012). The importance of soil can be reflected in bacterial richness and diversity
464 compared to pore spaces filled with water (Banerjee et al., 2016). On the other hand,
465 increasing soil moisture provides the microorganisms with essential substrates such as
466 ammonium, nitrate, and soluble organic carbon, and increases gas diffusion rates in the
467 water (Blagodatsky and Smith, 2012). Biologically available nitrogen often limit marine
468 productivity (Bertics et al., 2010), and thus can affect CO₂ fluxes to the atmosphere.

469 However, a mangrove fertilization experiment showed that CH₄ emission rates were not
470 affected by N addition (Kreuzwieser et al., 2003). A higher concentration of C_{mic} and
471 N_{mic} in the dry period (Table 2), both in the high and low topographies, indicated that
472 microorganisms are more active when the soil spends more time aerated in the dry
473 period (Table 2), time when only the high tides produce anoxia in the mangrove soil
474 mainly in the low topography. Under reduced oxygen conditions, in a laboratory
475 incubated mangrove soil, the addition of nitrogen resulted in a significant increase in the
476 microbial metabolic quotient, showing no concomitant change in microbial respiration,
477 which was explained by a decrease in microbial biomass (Craig et al., 2021).

478 The high OM concentration at the two topographic locations (Table 2), at the two
479 seasons studied, and the respective negative correlation with CO₂ flux (Table 5) confirm
480 the importance of microbial activity in mangrove soils (Gao et al., 2020). Also, CH₄
481 produced in flooded soils can be converted mainly to CO₂ by the anaerobic oxidation of
482 CH₄ (Boetius et al., 2000; Milucka et al., 2015; Xu et al., 2015) which may contribute to
483 the higher CO₂ efflux in the Mojuim River estuary compared to other tropical
484 mangroves (Rosentreter et al., 2018b). The belowground C stock is considered the
485 largest C reservoir in a mangrove ecosystem, and it results from the low OM
486 decomposition rate due to flooding (Marchand, 2017).

487 The higher water salinity influenced by the tidal movement in the dry season (Table 1)
488 seems to result in a lower CH₄ flux at the low topography (Dutta et al., 2013; Lekphet et
489 al., 2005; Shiau and Chiu, 2020). High SO₄²⁻ concentration in the marine sediments
490 inhibits methane formation due to competition between SO₄²⁻ reduction and
491 methanogenic fermentation, as sulfate-reducing bacteria are more efficient at using
492 hydrogen than methanotrophic bacteria (Abram and Nedwell, 1978; Kristjansson et al.,
493 1982), a key factor fostering reduced CH₄ emissions. At high SO₄²⁻ concentrations
494 methanotrophic bacteria use CH₄ as an energy source and oxidize it to CO₂ (Coyne,
495 1999; Segarra et al., 2015), increasing the efflux of CO₂ and reduced CH₄ (Megonigal
496 and Schlesinger, 2002; Roslev and King, 1996). This may explain the high CO₂ and low
497 CH₄ efflux found throughout the year at the high and, especially, at the low
498 topographies (Figure 3).

499 Studies in coastal ecosystems in Taiwan have reported that methanotrophic bacteria can
500 be sensitive to soil pH, and reported an optimal growth at pH ranging from 6.5 to 7.5
501 (Shiau et al., 2018). The higher soil acidity in the Mojuim River wetland (Table 1) may

502 be inhibiting the activity of methanogenic bacteria by increasing the population of
503 methanotrophic bacteria, which are efficient in CH₄ consumption (Chen et al., 2010;
504 Hegde et al., 2003; Shiau and Chiu, 2020). In addition, the pneumatophores present in
505 *R. mangle* increase soil aeration and reduce CH₄ emissions (Allen et al., 2011; He et al.,
506 2019). Spatial differences (topography) in CH₄ emissions in the soil can be attributed to
507 substrate heterogeneity, salinity, and the abundance of methanogenic and
508 methanotrophic bacteria (Gao et al., 2020). Increases in CH₄ efflux with reduced
509 salinity were found as a consequence of intense oxidation or reduced competition from
510 the more energetically efficient SO₄²⁻ and NO³⁻ reducing bacteria when compared to the
511 methanogenic bacteria (Biswas et al., 2007). This fact can be observed in the CH₄ efflux
512 in the mangrove of the Mojuim River, because there was an increased CH₄ production
513 especially in the low topography in the rainy season (Figure 3), when water salinity is
514 reduced (Table 1) due to the increased precipitation. However, we did not find a
515 correlation between CH₄ efflux and salinity, as previously reported (Purvaja and
516 Ramesh, 2001). ~~More detailed studies on CH₄ efflux and on its relationship with
517 methanotrophic bacteria and abiotic factors (mainly ammonia and sulfate) are needed
518 due to the average flux of 4.70 mg C m⁻² h⁻¹ and the extreme monthly and seasonal
519 variations.~~

520 5 Conclusions

521 Seasonality was important for CH₄ efflux but did not influence CO₂ efflux. The
522 differences in fluxes may be an effect of global climate changes on the terrestrial
523 biogeochemistry at the plant-soil-atmosphere interface, as indicated by the deviation in
524 precipitation values from the climatology normal, making it necessary to extend this
525 study for more years. Using the factor of 23 to convert the global warming potential of
526 CH₄ to CO₂ (IPCC, 2001), the CO₂ equivalent emission was 35.4 Mg CO₂-eq ha⁻¹ yr⁻¹.
527 Over a 100-year time period, a radiative forcing due to the continuous emission of 0.05
528 kg CH₄ m⁻² y⁻¹ found in this study, would be offset if CO₂ sequestration rates were 2.16
529 kg CO₂ m⁻² y⁻¹ (Neubauer and Megonigal, 2015).

530 Microtopography should be considered when determining the efflux of CO₂ and CH₄ in
531 mangrove forests in an Amazon estuary. The low topography in the mangrove forest of
532 Mojuim River had a higher concentration of organic carbon in the soil. However, it did
533 not produce a higher CO₂ efflux because it was negatively influenced by soil moisture,
534 which was indifferent to CH₄ efflux. MO, C/N ratio, and Eh were critical in soil

535 microbial activity, which resulted in a variation in CO₂ flux during the year and
536 seasonal periods. Thus, the physicochemical properties of the soil are important for CO₂
537 flux, especially in the rainy season. Still, they did not influence CH₄ fluxes.

538 *Data availability:* The data used in this article belong to the doctoral thesis of Saul
539 Castellón, within the Postgraduate Program in Environmental Sciences, at the Federal
540 University of Pará. Access to the data can be requested from Dr. Castellón
541 (saulmarz22@gmail.com), which holds the set of all data used in this paper.

542 *Author contributions:* SEMC and JHC designed the study and wrote the article with the
543 help of JFB, MR, MLR, and CN. JFB assisted in the field experiment. MR provided
544 logistical support in field activities.

545 *Competing interests:* The authors declare that they have no conflict of interest

546 *Acknowledgements:* The authors are grateful to the Program of Alliances for Education
547 and Training of the Organization of the American States and to Coimbra Group of
548 Brazilian Universities, for the financial support, as well as to Paulo Sarmento for the
549 assistance at laboratory analysis, and to Maridalva Ribeiro and Lucivaldo da Silva for
550 the fieldwork assistance. Furthermore, the authors would like to thank the Laboratory of
551 Biogeochemical Cycles (Geosciences Institute, Federal University of Pará) for the
552 equipment provided for this research.

553 6 References

554 Abram, J. W. and Nedwell, D. B.: Inhibition of methanogenesis by sulphate reducing
555 bacteria competing for transferred hydrogen, *Arch. Microbiol.*, 117(1), 89–92,
556 doi:10.1007/BF00689356, 1978.

557 Adame, M. F., Connolly, R. M., Turschwell, M. P., Lovelock, C. E., Fatoyinbo, T.,
558 Lagomasino, D., Goldberg, L. A., Holdorf, J., Friess, D. A., Sasmito, S. D., Sanderman,
559 J., Sievers, M., Buelow, C., Kauffman, J. B., Bryan-Brown, D. and Brown, C. J.: Future
560 carbon emissions from global mangrove forest loss, *Glob. Chang. Biol.*, 27(12), 2856–
561 2866, doi:10.1111/gcb.15571, 2021.

562 Allen, D., Dalal, R. C., Rennenberg, H. and Schmidt, S.: Seasonal variation in nitrous
563 oxide and methane emissions from subtropical estuary and coastal mangrove sediments,
564 Australia, *Plant Biol.*, 13(1), 126–133, doi:10.1111/j.1438-8677.2010.00331.x, 2011.

565 Almeida, R. F. de, Mikhael, J. E. R., Franco, F. O., Santana, L. M. F. and Wendling, B.:

566 Measuring the labile and recalcitrant pools of carbon and nitrogen in forested and
567 agricultural soils: A study under tropical conditions, *Forests*, 10(7), 544,
568 doi:10.3390/f10070544, 2019.

569 Alongi, D. M.: The contribution of mangrove ecosystems to global carbon cycling and
570 greenhouse gas emissions, in *Greenhouse gas and carbon balances in mangrove coastal*
571 *ecosystems*, edited by Y. Tateda, R. Upstill-Goddard, T. Goreau, D. M. Alongi, A.
572 Nose, E. Kristensen, and G. Wattayakorn, pp. 1–10, Gendai Tosh, Kanagawa, Japan.,
573 2007.

574 Alongi, D. M.: *The Energetics of Mangrove Forests*, Springer Netherlands, Dordrecht.,
575 2009.

576 Alongi, D. M. and Christoffersen, P.: Benthic infauna and organism-sediment relations
577 in a shallow, tropical coastal area: influence of outwelled mangrove detritus and
578 physical disturbance, *Mar. Ecol. Prog. Ser.*, 81(3), 229–245, doi:10.3354/meps081229,
579 1992.

580 Alongi, D. M. and Mukhopadhyay, S. K.: Contribution of mangroves to coastal carbon
581 cycling in low latitude seas, *Agric. For. Meteorol.*, 213, 266–272,
582 doi:10.1016/j.agrformet.2014.10.005, 2015.

583 Angelov, M. N., Sung, S. J. S., Doong, R. Lou, Harms, W. R., Kormanik, P. P. and
584 Black, C. C.: Long-and short-term flooding effects on survival and sink-source
585 relationships of swamp-adapted tree species, *Tree Physiol.*, 16(4), 477–484,
586 doi:10.1093/treephys/16.5.477, 1996.

587 Araujo, A. S. F. de: Is the microwave irradiation a suitable method for measuring soil
588 microbial biomass?, *Rev. Environ. Sci. Biotechnol.*, 9(4), 317–321,
589 doi:10.1007/s11157-010-9210-y, 2010.

590 Banerjee, S., Helgason, B., Wang, L., Winsley, T., Ferrari, B. C. and Siciliano, S. D.:
591 Legacy effects of soil moisture on microbial community structure and N₂O emissions,
592 *Soil Biol. Biochem.*, 95, 40–50, doi:10.1016/j.soilbio.2015.12.004, 2016.

593 Bastviken, D., Tranvik, L. J., Downing, J. A., Crill, P. M. and Enrich-Prast, A.:
594 Freshwater Methane Emissions Offset the Continental Carbon Sink, *Science* (80-.),
595 331(6013), 50–50, doi:10.1126/science.1196808, 2011.

596 Bauza, J. F., Morell, J. M. and Corredor, J. E.: Biogeochemistry of Nitrous Oxide

597 Production in the Red Mangrove (*Rhizophora mangle*) Forest Sediments, *Estuar. Coast.*
598 *Shelf Sci.*, 55(5), 697–704, doi:10.1006/ECSS.2001.0913, 2002.

599 Bertics, V. J., Sohm, J. A., Treude, T., Chow, C. E. T., Capone, D. G., Fuhrman, J. A.
600 and Ziebis, W.: Burrowing deeper into benthic nitrogen cycling: The impact of
601 Bioturbation on nitrogen fixation coupled to sulfate reduction, *Mar. Ecol. Prog. Ser.*,
602 409, 1–15, doi:10.3354/meps08639, 2010.

603 Biswas, H., Mukhopadhyay, S. K., Sen, S. and Jana, T. K.: Spatial and temporal
604 patterns of methane dynamics in the tropical mangrove dominated estuary, NE coast of
605 Bay of Bengal, India, *J. Mar. Syst.*, 68(1–2), 55–64, doi:10.1016/j.jmarsys.2006.11.001,
606 2007.

607 Blagodatsky, S. and Smith, P.: Soil physics meets soil biology: Towards better
608 mechanistic prediction of greenhouse gas emissions from soil, *Soil Biol. Biochem.*, 47,
609 78–92, doi:10.1016/J.SOILBIO.2011.12.015, 2012.

610 Boetius, A., Ravenschlag, K., Schubert, C. J., Rickert, D., Widdel, F., Gieseke, A.,
611 Amann, R., Jørgensen, B. B., Witte, U. and Pfannkuche, O.: A marine microbial
612 consortium apparently mediating anaerobic oxidation methane, *Nature*, 407(6804), 623–
613 626, doi:10.1038/35036572, 2000.

614 Borges, A. V., Abril, G., Darchambeau, F., Teodoro, C. R., Deborde, J., Vidal, L. O.,
615 Lambert, T. and Bouillon, S.: Divergent biophysical controls of aquatic CO₂ and CH₄
616 in the World's two largest rivers, *Sci. Rep.*, 5, doi:10.1038/srep15614, 2015.

617 Borges, A. V., Abril, G. and Bouillon, S.: Carbon dynamics and CO₂ and CH₄
618 outgassing in the Mekong delta, *Biogeosciences*, 15(4), 1093–1114, doi:10.5194/bg-15-
619 1093-2018, 2018.

620 Bouillon, S., Borges, A. V., Castañeda-Moya, E., Diele, K., Dittmar, T., Duke, N. C.,
621 Kristensen, E., Lee, S. Y., Marchand, C., Middelburg, J. J., Rivera-Monroy, V. H.,
622 Smith, T. J. and Twilley, R. R.: Mangrove production and carbon sinks: A revision of
623 global budget estimates, *Global Biogeochem. Cycles*, 22(2), 1–12,
624 doi:10.1029/2007GB003052, 2008.

625 Brookes, P. C., Landman, A., Pruden, G. and Jenkinson, D. S.: Chloroform fumigation
626 and the release of soil nitrogen: A rapid direct extraction method to measure microbial
627 biomass nitrogen in soil, *Soil Biol. Biochem.*, 17(6), 837–842, doi:10.1016/0038-

628 0717(85)90144-0, 1985.

629 Cameron, C., Hutley, L. B., Munksgaard, N. C., Phan, S., Aung, T., Thinn, T., Aye, W.
630 M. and Lovelock, C. E.: Impact of an extreme monsoon on CO₂ and CH₄ fluxes from
631 mangrove soils of the Ayeyarwady Delta, Myanmar, *Sci. Total Environ.*, 760, 143422,
632 doi:10.1016/j.scitotenv.2020.143422, 2021.

633 Castillo, J. A. A., Apan, A. A., Maraseni, T. N. and Salmo, S. G.: Soil greenhouse gas
634 fluxes in tropical mangrove forests and in land uses on deforested mangrove lands,
635 *Catena*, 159, 60–69, doi:10.1016/j.catena.2017.08.005, 2017.

636 Chanda, A., Akhand, A., Manna, S., Dutta, S., Das, I., Hazra, S., Rao, K. H. and
637 Dadhwal, V. K.: Measuring daytime CO₂ fluxes from the inter-tidal mangrove soils of
638 Indian Sundarbans, *Environ. Earth Sci.*, 72(2), 417–427, doi:10.1007/s12665-013-2962-
639 2, 2014.

640 Chauhan, R., Datta, A., Ramanathan, A. and Adhya, T. K.: Factors influencing spatio-
641 temporal variation of methane and nitrous oxide emission from a tropical mangrove of
642 eastern coast of India, *Atmos. Environ.*, 107, 95–106,
643 doi:10.1016/j.atmosenv.2015.02.006, 2015.

644 Chen, G. C., Tam, N. F. Y. and Ye, Y.: Spatial and seasonal variations of atmospheric
645 N₂O and CO₂ fluxes from a subtropical mangrove swamp and their relationships with
646 soil characteristics, *Soil Biol. Biochem.*, 48, 175–181,
647 doi:10.1016/j.soilbio.2012.01.029, 2012.

648 Chen, G. C., Ulumuddin, Y. I., Pramudji, S., Chen, S. Y., Chen, B., Ye, Y., Ou, D. Y.,
649 Ma, Z. Y., Huang, H. and Wang, J. K.: Rich soil carbon and nitrogen but low
650 atmospheric greenhouse gas fluxes from North Sulawesi mangrove swamps in
651 Indonesia, *Sci. Total Environ.*, 487(1), 91–96, doi:10.1016/j.scitotenv.2014.03.140,
652 2014.

653 Chen, G. C. C., Tam, N. F. Y. F. Y. and Ye, Y.: Summer fluxes of atmospheric
654 greenhouse gases N₂O, CH₄ and CO₂ from mangrove soil in South China, *Sci. Total
655 Environ.*, 408(13), 2761–2767, doi:10.1016/j.scitotenv.2010.03.007, 2010.

656 Chowdhury, T. R., Bramer, L., Hoyt, D. W., Kim, Y. M., Metz, T. O., McCue, L. A.,
657 Diefenderfer, H. L., Jansson, J. K. and Bailey, V.: Temporal dynamics of CO₂ and CH₄
658 loss potentials in response to rapid hydrological shifts in tidal freshwater wetland soils,

659 Ecol. Eng., 114, 104–114, doi:10.1016/j.ecoleng.2017.06.041, 2018.

660 Chuang, P. C., Young, M. B., Dale, A. W., Miller, L. G., Herrera-Silveira, J. A. and
661 Paytan, A.: Methane and sulfate dynamics in sediments from mangrove-dominated
662 tropical coastal lagoons, Yucatan, Mexico, Biogeosciences, 13(10), 2981–3001, 2016.

663 Coyne, M.: Soil Microbiology: An Exploratory Approach, Delmar Publishers, New
664 York, NY, USA., 1999.

665 Craig, H., Antwis, R. E., Cordero, I., Ashworth, D., Robinson, C. H., Osborne, T. Z.,
666 Bardgett, R. D., Rowntree, J. K. and Simpson, L. T.: Nitrogen addition alters
667 composition, diversity, and functioning of microbial communities in mangrove soils:
668 An incubation experiment, Soil Biol. Biochem., 153, 108076,
669 doi:10.1016/j.soilbio.2020.108076, 2021.

670 Dai, Z., Trettin, C. C., Li, C., Li, H., Sun, G. and Amatya, D. M.: Effect of Assessment
671 Scale on Spatial and Temporal Variations in CH₄, CO₂, and N₂O Fluxes in a Forested
672 Wetland, Water, Air, Soil Pollut., 223(1), 253–265, doi:10.1007/s11270-011-0855-0,
673 2012.

674 Davidson, E. A., Verchot, L. V., Cattanio, J. H., Ackerman, I. L. and Carvalho, J. E. M.:
675 Effects of soil water content on soil respiration in forests and cattle pastures of eastern
676 Amazonia, Biogeochemistry, 48(1), 53–69, doi:10.1023/a:1006204113917, 2000.

677 Donato, D. C., Kauffman, J. B., Murdiyarso, D., Kurnianto, S., Stidham, M. and
678 Kanninen, M.: Mangroves among the most carbon-rich forests in the tropics, Nat.
679 Geosci., 4(5), 293–297, doi:10.1038/ngeo1123, 2011.

680 Dutta, M. K., Chowdhury, C., Jana, T. K. and Mukhopadhyay, S. K.: Dynamics and
681 exchange fluxes of methane in the estuarine mangrove environment of the Sundarbans,
682 NE coast of India, Atmos. Environ., 77, 631–639, doi:10.1016/j.atmosenv.2013.05.050,
683 2013.

684 Ehrenfeld, J. G.: Microsite differences in surface substrate characteristics in
685 Chamaecyparis swamps of the New Jersey Pinelands, Wetlands, 15(2), 183–189,
686 doi:10.1007/BF03160672, 1995.

687 El-Robrini, M., Alves, M. A. M. S., Souza Filho, P. W. M., El-Robrini M. H. S., Silva
688 Júnior, O. G. and França, C. F.: Atlas de Erosão e Progradação da zona costeira do
689 Estado do Pará – Região Amazônica: Áreas oceânica e estuarina, in Atlas de Erosão e

690 Progradação da Zona Costeira Brasileira, edited by D. Muehe, pp. 1–34, São Paulo.,
691 2006.

692 EPA, E. P. A.: Inventory of U.S. Greenhouse Gas Emissions and Sinks: 1990–2015.,
693 2017.

694 Fernandes, W. A. A. and Pimentel, M. A. da S.: Dinâmica da paisagem no entorno da
695 RESEX marinha de São João da Ponta/PA: utilização de métricas e geoprocessamento,
696 Caminhos Geogr., 20(72), 326–344, doi:10.14393/RCG207247140, 2019.

697 Ferreira, A. S., Camargo, F. A. O. and Vidor, C.: Utilização de microondas na avaliação
698 da biomassa microbiana do solo, Rev. Bras. Ciência do Solo, 23(4), 991–996,
699 doi:10.1590/S0100-06831999000400026, 1999.

700 Ferreira, S. da S.: Entre marés e mangues: paisagens territorializadas por pescadores da
701 resex marinha de São João da Ponta (PA), Federal University of Pará., 2017.

702 França, C. F. de, Pimentel, M. A. D. S. and Neves, S. C. R.: Estrutura Paisagística De
703 São João Da Ponta, Nordeste Do Pará, Geogr. Ensino Pesqui., 20(1), 130–142,
704 doi:10.5902/2236499418331, 2016.

705 Frankignoulle, M.: Field measurements of air-sea CO₂ exchange, Limnol. Oceanogr.,
706 33(3), 313–322, 1988.

707 Friesen, S. D., Dunn, C. and Freeman, C.: Decomposition as a regulator of carbon
708 accretion in mangroves: a review, Ecol. Eng., 114, 173–178,
709 doi:10.1016/j.ecoleng.2017.06.069, 2018.

710 Fromard, F., Puig, H., Cadamuro, L., Marty, G., Betoulle, J. L. and Mougin, E.:
711 Structure, above-ground biomass and dynamics of mangrove ecosystems: new data
712 from French Guiana, Oecologia, 115(1), 39–53, doi:10.1007/s004420050489, 1998.

713 Gao, G. F., Zhang, X. M., Li, P. F., Simon, M., Shen, Z. J., Chen, J., Gao, C. H. and
714 Zheng, H. L.: Examining Soil Carbon Gas (CO₂, CH₄) Emissions and the Effect on
715 Functional Microbial Abundances in the Zhangjiang Estuary Mangrove Reserve, J.
716 Coast. Res., 36(1), 54–62, doi:10.2112/JCOASTRES-D-18-00107.1, 2020.

717 Gardunho, D. C. L.: Estimativas de biomassa acima do solo da floresta de mangue na
718 península de Ajuruteua, Bragança – PA, Federal University of Pará, Belém, Brazil.,
719 2017.

720 Gash, J. H. C., Huntingford, C., Marengo, J. A., Betts, R. A., Cox, P. M., Fisch, G., Fu,
721 R., Gandu, A. W., Harris, P. P., Machado, L. A. T., von Randow, C. and Silva Dias, M.
722 A.: Amazonian climate: Results and future research, *Theor. Appl. Climatol.*, 78(1–3),
723 187–193, doi:10.1007/s00704-004-0052-9, 2004.

724 Hamilton, S. E. and Friess, D. A.: Global carbon stocks and potential emissions due to
725 mangrove deforestation from 2000 to 2012, *Nat. Clim. Chang.*, 8(3), 240–244,
726 doi:10.1038/s41558-018-0090-4, 2018.

727 He, Y., Guan, W., Xue, D., Liu, L., Peng, C., Liao, B., Hu, J., Zhu, Q., Yang, Y., Wang,
728 X., Zhou, G., Wu, Z. and Chen, H.: Comparison of methane emissions among invasive
729 and native mangrove species in Dongzhaigang, Hainan Island, *Sci. Total Environ.*, 697,
730 133945, doi:10.1016/j.scitotenv.2019.133945, 2019.

731 Hegde, U., Chang, T.-C. and Yang, S.-S.: Methane and carbon dioxide emissions from
732 Shan-Chu-Ku landfill site in northern Taiwan., *Chemosphere*, 52(8), 1275–1285,
733 doi:10.1016/S0045-6535(03)00352-7, 2003.

734 Herz, R.: Manguezais do Brasil, Instituto Oceanografico da USP/CIRM, São Paulo,
735 Brazil., 1991.

736 Howard, J., Hoyt, S., Isensee, K., Telszewski, M. and Pidgeon, E.: Coastal Blue
737 Carbon: Methods for Assessing Carbon Stocks and Emissions Factors in Mangroves,
738 Tidal Salt Marshes, and Seagrasses, edited by J. Howard, S. Hoyt, K. Isensee, M.
739 Telszewski, and E. Pidgeon, International Union for Conservation of Nature, Arlington,
740 Virginia, USA. [online] Available from:
741 http://www.cifor.org/publications/pdf_files/Books/BMurdiyarso1401.pdf (Accessed 11
742 September 2019), 2014.

743 IPCC: Climate Change 2001: Third Assessment Report of the IPCC, Cambridge., 2001.

744 Islam, K. R. and Weil, R. R.: Microwave irradiation of soil for routine measurement of
745 microbial biomass carbon, *Biol. Fertil. Soils*, 27(4), 408–416,
746 doi:10.1007/s003740050451, 1998.

747 Kalembasa, S. J. and Jenkinson, D. S.: A comparative study of titrimetric and
748 gavimetric methods for determination of organic carbon in soil, *J. Sci. Food Agric.*, 24,
749 1085–1090, 1973.

750 Kauffman, B. J., Donato, D. and Adame, M. F.: Protocolo para la medición, monitoreo

751 y reporte de la estructura, biomasa y reservas de carbono de los manglares, Bogor,
752 Indonesia., 2013.

753 Kauffman, J. B., Bernardino, A. F., Ferreira, T. O., Giovannoni, L. R., de O. Gomes, L.
754 E., Romero, D. J., Jimenez, L. C. Z. and Ruiz, F.: Carbon stocks of mangroves and salt
755 marshes of the Amazon region, Brazil, *Biol. Lett.*, 14(9), 20180208,
756 doi:10.1098/rsbl.2018.0208, 2018.

757 Kreuzwieser, J., Buchholz, J. and Rennenberg, H.: Emission of Methane and Nitrous
758 Oxide by Australian Mangrove Ecosystems, *Plant Biol.*, 5(4), 423–431, doi:10.1055/s-
759 2003-42712, 2003.

760 Kristensen, E., Bouillon, S., Dittmar, T. and Marchand, C.: Organic carbon dynamics in
761 mangrove ecosystems: A review, *Aquat. Bot.*, 89(2), 201–219,
762 doi:10.1016/J.AQUABOT.2007.12.005, 2008.

763 Kristjansson, J. K., Schönheit, P. and Thauer, R. K.: Different Ks values for hydrogen
764 of methanogenic bacteria and sulfate reducing bacteria: An explanation for the apparent
765 inhibition of methanogenesis by sulfate, *Arch. Microbiol.*, 131(3), 278–282,
766 doi:10.1007/BF00405893, 1982.

767 Lekphet, S., Nitisoravut, S. and Adsavakulchai, S.: Estimating methane emissions from
768 mangrove area in Ranong Province, Thailand, *Songklanakarin J. Sci. Technol.*, 27(1),
769 153–163 [online] Available from: <https://www.researchgate.net/publication/26473398>
770 (Accessed 29 January 2019), 2005.

771 Maher, D. T., Call, M., Santos, I. R. and Sanders, C. J.: Beyond burial: Lateral
772 exchange is a significant atmospheric carbon sink in mangrove forests, *Biol. Lett.*,
773 14(7), 1–4, doi:10.1098/rsbl.2018.0200, 2018.

774 Mahesh, P., Sreenivas, G., Rao, P. V. N. N., Dadhwal, V. K., Sai Krishna, S. V. S. S.
775 and Mallikarjun, K.: High-precision surface-level CO₂ and CH₄ using off-axis
776 integrated cavity output spectroscopy (OA-ICOS) over Shadnagar, India, *Int. J. Remote
777 Sens.*, 36(22), 5754–5765, doi:10.1080/01431161.2015.1104744, 2015.

778 Marchand, C.: Soil carbon stocks and burial rates along a mangrove forest
779 chronosequence (French Guiana), *For. Ecol. Manage.*, 384, 92–99,
780 doi:10.1016/j.foreco.2016.10.030, 2017.

781 McEwing, K. R., Fisher, J. P. and Zona, D.: Environmental and vegetation controls on

782 the spatial variability of CH₄ emission from wet-sedge and tussock tundra ecosystems
783 in the Arctic, *Plant Soil*, 388(1–2), 37–52, doi:10.1007/s11104-014-2377-1, 2015.

784 Megonigal, J. P. and Schlesinger, W. H.: Methane-limited methanotrophy in tidal
785 freshwater swamps, *Global Biogeochem. Cycles*, 16(4), 35-1-35-10,
786 doi:10.1029/2001GB001594, 2002.

787 Menezes, M. P. M. de, Berger, U. and Mehlig, U.: Mangrove vegetation in Amazonia :
788 a review of studies from the coast of Pará and Maranhão States , north Brazil, *Acta*
789 *Amaz.*, 38(3), 403–420, doi:10.1590/S0044-59672008000300004, 2008.

790 Milucka, J., Kirf, M., Lu, L., Krupke, A., Lam, P., Littmann, S., Kuypers, M. M. M. and
791 Schubert, C. J.: Methane oxidation coupled to oxygenic photosynthesis in anoxic
792 waters, *ISME J.*, 9(9), 1991–2002, doi:10.1038/ismej.2015.12, 2015.

793 Monz, C. A., Reuss, D. E. and Elliott, E. T.: Soil microbial biomass carbon and nitrogen
794 estimates using 2450 MHz microwave irradiation or chloroform fumigation followed by
795 direct extraction, *Agric. Ecosyst. Environ.*, 34(1–4), 55–63, doi:10.1016/0167-
796 8809(91)90093-D, 1991.

797 Neubauer, S. C. and Megonigal, J. P.: Moving Beyond Global Warming Potentials to
798 Quantify the Climatic Role of Ecosystems, *Ecosystems*, 18(6), 1000–1013,
799 doi:10.1007/S10021-015-9879-4/TABLES/2, 2015.

800 Nóbrega, G. N., Ferreira, T. O., Siqueira Neto, M., Queiroz, H. M., Artur, A. G.,
801 Mendonça, E. D. S., Silva, E. D. O. and Otero, X. L.: Edaphic factors controlling
802 summer (rainy season) greenhouse gas emissions (CO₂ and CH₄) from semiarid
803 mangrove soils (NE-Brazil), *Sci. Total Environ.*, 542, 685–693,
804 doi:10.1016/j.scitotenv.2015.10.108, 2016.

805 Norman, J. M., Kucharik, C. J., Gower, S. T., Baldocchi, D. D., Crill, P. M., Rayment,
806 M., Savage, K. and Striegl, R. G.: A comparison of six methods for measuring soil-
807 surface carbon dioxide fluxes, *J. Geophys. Res. Atmos.*, 102(D24), 28771–28777,
808 doi:10.1029/97JD01440, 1997.

809 Peel, M. C., Finlayson, B. L. and McMahon, T. A.: Updated world map of the Köppen-
810 Geiger climate classification, *Hydrol. Earth Syst. Sci.*, 11(5), 1633–1644,
811 doi:10.1002/ppp.421, 2007.

812 Poffenbarger, H. J., Needelman, B. A. and Megonigal, J. P.: Salinity Influence on

813 Methane Emissions from Tidal Marshes, Wetlands, 31(5), 831–842,
814 doi:10.1007/s13157-011-0197-0, 2011.

815 Prost, M. T., Mendes, A. C., Faure, J. F., Berredo, J. F., Sales, M. E. ., Furtado, L. G.,
816 Santana, M. G., Silva, C. A., Nascimento, I. ., Gorayeb, I., Secco, M. F. and Luz, L.:
817 Manguezais e estuários da costa paraense: exemplo de estudo multidisciplinar integrado
818 (Marapanim e São Caetano de Odivelas), in Ecossistemas Costeiros: Impactos e Gestão
819 Ambiental, edited by M. T. Prost and A. Mendes, pp. 25–52, FUNTEC and Paraense
820 Museum “Emílio Goeldi,” Belém, Brazil., 2001.

821 Purvaja, R. and Ramesh, R.: Natural and Anthropogenic Methane Emission from
822 Coastal Wetlands of South India, Environ. Manage., 27(4), 547–557,
823 doi:10.1007/s002670010169, 2001.

824 Purvaja, R., Ramesh, R. and Frenzel, P.: Plant-mediated methane emission from an
825 Indian mangrove, Glob. Chang. Biol., 10(11), 1825–1834, doi:10.1111/j.1365-
826 2486.2004.00834.x, 2004.

827 Reeburgh, W. S.: Oceanic Methane Biogeochemistry, Chem. Rev., 2, 486–513,
828 doi:10.1021/cr050362v, 2007.

829 Robertson, A. I., Alongi, D. M. and Boto, K. G.: Food chains and carbon fluxes, in
830 Coastal and Estuarine Studies, edited by A. I. Robertson and D. M. Alongi, pp. 293–
831 326, American Geophysical Union., 1992.

832 Rocha, A. S.: Caracterização física do estuário do rio Mojuim em São Caetano de
833 Odivelas - PA, Federal University of Pará. [online] Available from:
834 <http://repositorio.ufpa.br/jspui/handle/2011/11390>, 2015.

835 Rollnic, M., Costa, M. S., Medeiros, P. R. L. and Monteiro, S. M.: Tide Influence on
836 Suspended Matter Transport in an Amazonian Estuary, J. Coast. Res., 85, 121–125,
837 doi:10.2112/SI85-025.1, 2018.

838 Rosentreter, J. A., Maher, D. T., Erler, D. V., Murray, R. H. and Eyre, B. D.: Methane
839 emissions partially offset “blue carbon” burial in mangroves, Sci. Adv., 4(6), 1–11,
840 doi:10.1126/sciadv.aoa4985, 2018a.

841 Rosentreter, J. A., Maher, D. . T., Erler, D. V. V., Murray, R. and Eyre, B. D. D.:
842 Seasonal and temporal CO₂ dynamics in three tropical mangrove creeks – A revision of
843 global mangrove CO₂ emissions, Geochim. Cosmochim. Acta, 222, 729–745,

844 doi:10.1016/j.gca.2017.11.026, 2018b.

845 Roslev, P. and King, G. M.: Regulation of methane oxidation in a freshwater wetland by
846 water table changes and anoxia, *FEMS Microbiol. Ecol.*, 19(2), 105–115,
847 doi:10.1111/j.1574-6941.1996.tb00203.x, 1996.

848 Sahu, S. K. and Kathiresan, K.: The age and species composition of mangrove forest
849 directly influence the net primary productivity and carbon sequestration potential,
850 *Biocatal. Agric. Biotechnol.*, 20, 101235, doi:10.1016/j.bcab.2019.101235, 2019.

851 Salum, R. B., Souza-Filho, P. W. M., Simard, M., Silva, C. A., Fernandes, M. E. B.,
852 Cougo, M. F., do Nascimento, W. and Rogers, K.: Improving mangrove above-ground
853 biomass estimates using LiDAR, *Estuar. Coast. Shelf Sci.*, 236, 106585,
854 doi:10.1016/j.ecss.2020.106585, 2020.

855 Schmidt, M. W. I., Torn, M. S., Abiven, S., Dittmar, T., Guggenberger, G., Janssens, I.
856 A., Kleber, M., Kögel-Knabner, I., Lehmann, J., Manning, D. A. C., Nannipieri, P.,
857 Rasse, D. P., Weiner, S. and Trumbore, S. E.: Persistence of soil organic matter as an
858 ecosystem property, *Nature*, 478(7367), 49–56, doi:10.1038/nature10386, 2011.

859 Segarra, K. E. A., Schubotz, F., Samarkin, V., Yoshinaga, M. Y., Hinrichs, K. U. and
860 Joye, S. B.: High rates of anaerobic methane oxidation in freshwater wetlands reduce
861 potential atmospheric methane emissions, *Nat. Commun.*, 6(1), 1–8,
862 doi:10.1038/ncomms8477, 2015.

863 Shiau, Y.-J. and Chiu, C.-Y.: Biogeochemical Processes of C and N in the Soil of
864 Mangrove Forest Ecosystems, *Forests*, 11(5), 492, doi:10.3390/f11050492, 2020.

865 Shiau, Y. J., Cai, Y., Lin, Y. Te, Jia, Z. and Chiu, C. Y.: Community Structure of Active
866 Aerobic Methanotrophs in Red Mangrove (*Kandelia obovata*) Soils Under Different
867 Frequency of Tides, *Microb. Ecol.*, 75(3), 761–770, doi:10.1007/s00248-017-1080-1,
868 2018.

869 Sihi, D., Davidson, E. A., Chen, M., Savage, K. E., Richardson, A. D., Keenan, T. F.
870 and Hollinger, D. Y.: Merging a mechanistic enzymatic model of soil heterotrophic
871 respiration into an ecosystem model in two AmeriFlux sites of northeastern USA,
872 *Agric. For. Meteorol.*, 252, 155–166, doi:10.1016/J.AGRFORMAT.2018.01.026, 2018.

873 Souza Filho, P. W. M.: Costa de manguezais de macromaré da Amazônia: cenários
874 morfológicos, mapeamento e quantificação de áreas usando dados de sensores remotos,

875 Rev. Bras. Geofísica, 23(4), 427–435, doi:10.1590/S0102-261X2005000400006, 2005.

876 Sparling, G. P. and West, A. W.: A direct extraction method to estimate soil microbial
877 C: calibration in situ using microbial respiration and ^{14}C labelled cells, Soil Biol.
878 Biochem., 20(3), 337–343, doi:10.1016/0038-0717(88)90014-4, 1988.

879 Sundqvist, E., Vestin, P., Crill, P., Persson, T. and Lindroth, A.: Short-term effects of
880 thinning, clear-cutting and stump harvesting on methane exchange in a boreal forest,
881 Biogeosciences, 11(21), 6095–6105, doi:10.5194/bg-11-6095-2014, 2014.

882 Valentim, M., Monteiro, S. and Rollnic, M.: The Influence of Seasonality on Haline
883 Zones in An Amazonian Estuary, J. Coast. Res., 85, 76–80, doi:10.2112/SI85-016.1,
884 2018.

885 Valentine, D. L.: Emerging Topics in Marine Methane Biogeochemistry, Ann. Rev.
886 Mar. Sci., 3(1), 147–171, doi:10.1146/annurev-marine-120709-142734, 2011.

887 Vance, E. D., Brookes, P. C. and Jenkinson, D. S.: An extraction method for measuring
888 soil microbial biomass C, Soil Biol. Biochem., 19(6), 703–707, doi:10.1016/0038-
889 0717(87)90052-6, 1987.

890 Verchot, L. V., Davidson, E. A., Cattânia, J. H. and Ackerman, I. L.: Land-use change
891 and biogeochemical controls of methane fluxes in soils of eastern Amazonia,
892 Ecosystems, 3(1), 41–56, doi:10.1007/s100210000009, 2000.

893 Wang, X., Zhong, S., Bian, X. and Yu, L.: Impact of 2015–2016 El Niño and 2017–
894 2018 La Niña on PM2.5 concentrations across China, Atmos. Environ., 208, 61–73,
895 doi:10.1016/J.ATMOSENV.2019.03.035, 2019.

896 Whalen, S. C.: Biogeochemistry of Methane Exchange between Natural Wetlands and
897 the Atmosphere, Environ. Eng. Sci., 22(1), 73–94, doi:10.1089/ees.2005.22.73, 2005.

898 Xu, X., Elias, D. A., Graham, D. E., Phelps, T. J., Carroll, S. L., Wullschleger, S. D. and
899 Thornton, P. E.: A microbial functional group-based module for simulating methane
900 production and consumption: Application to an incubated permafrost soil, J. Geophys.
901 Res. Biogeosciences, 120(7), 1315–1333, doi:10.1002/2015JG002935, 2015.

902